Available online at www.sciencedirect.com

SciVerse ScienceDirect

Physics Procedia 36 (2012) 150 – 155

Physics Procedia

Superconductivity Centennial Conference

Prediction of Initiation Site of Destruction of Flat Braided Carbon Fiber Composites Using HTS-SQUID Gradiometer

Y. Shinyama[1]*, Y. Hatsukade[1], S. Tanaka[1], Y. Takai[2], M. S. Aly-Hassan[2], A. Nakai[2], H. Hamada[2]

[1]*Department of Environmental and Life Sciences, Toyohashi University of Technology, 1-1 Hibarigaoka, Tenpak0075-cho, Toyohashi, Aichi 441-8580, Japan*

[2]*Advanced Fibro-Science Division, Kyoto Institute of Technology, Matsugasaki, Sakyo-ku, Kyoto 606-8585 ,Japan*

Abstract

Carbon fiber reinforced polymers (CFRPs) are composite materials with lightweight and high specific strength. As the braided CFRPs have continuous carbon-fiber bundles in their longitudinal direction, they are stronger than conventional CFRPs. In this study, we applied a current-injection-based NDE method using a HTS-SQUID gradiometer to the flat braided CFRPs with and without carbon nanotubes (CNTs), and estimated conditions of the carbon fibers while applying a step-by-step tensile load to the CFRPs. From the results, a possibility to predict an initiation site of the destruction in the braided CFRPs was demonstrated.

PACS Codes: 85.25.Dq, 81.70.Ex, 81.70.-q

Keywords: NDE; HTS-SQUID; gradiometer; flat braided CFRP; current injection; tensile load

1. Introduction

Recently, braided carbon fiber reinforced polymers (CFRPs), in which carbon-fiber bundles are interlaced in a braided textile, have been developed and researched [1]. As the braided CFRPs have continuous carbon-fiber bundles in their longitudinal direction, they are stronger than conventional woven CFRPs, and application for industrial products are ongoing [2]. Because the strength of the braided CFRPs is maintained mainly by continuity of carbon fibers, a nondestructive evaluation (NDE) method,

* Corresponding author.
E-mail address: y083818@edu.imc.tut.ac.jp

 doi:10.1016/j.phpro.2012.06.062

which can detect breakage of the carbon fibers, is needed for practical use. Since the diameter of the carbon fibers in the braided CFRPs is several μm, it is difficult to detect breakage of the fibers by conventional NDE methods such as x-ray testing or ultrasonic testing. On the other hand, the electric conductivity of the carbon fibers changes considerably when they are broken. By applying a voltage to the braided CFRP, a current will flow in the carbon fibers according to the distribution of the electric conductivity in the braided CFRP. Therefore, by measuring the current distribution in the braided CFRP with a high sensitivity and high spatial resolution, the site where electric conductivity is different will be detected to evaluate the conditions of the carbon fibers. Therefore, we have developed a NDE method in which magnetic field gradients above board specimens were measured with superconducting quantum interference devise (SQUID) gradiometers to estimate current distributions in the specimens from the gradient distributions [3,4]. So far, we injected currents into braided CFRP specimens with artificial cracks, which cut one bundle or many bundles of the specimens, and measured generated magnetic field gradients with a high-temperature superconducting (HTS) SQUID gradiometer. From the results, it was estimated that a current in a braided CFRP flowed in low resistive bundles in the case of a normal braided CFRP, on the other hand, the current transmitted between the bundles through the contact points with the other healthy bundles in the case that continuous fibers were broken [3,4]. In this work, step-by-step tensile tests on braided CFRP specimens were carried out to make breakage of the braided CFRPs step by step, and magnetic field gradients were measured with the SQUID-NDE method at certain stages, and conditions of the fibers in the braided CFRPs were evaluated.

2. Specimens and tensile test

2.1. Specimens

Two kinds of flat braided CFRPs were prepared as specimens. Fig. 1 (a) shows a picture of a flat braided CFRP specimen. As the appearances of the specimens are similar, only the picture of one specimen is shown. These specimens consist of 25 carbon-fiber bundles (HTS40-12k, Toho Tenax) which were braided in a flat textile with angles of ±45°, and were fixed with epoxy resin (JER828, Japan Epoxy Resins Co. Ltd.). Fig. 1 (b) shows a photo of carbon nanotubes (CNTs) (Vapor grown carbon nanofiber, 10-20 μm length, 100-150 nm diameter, Showa Denko k.k.). CNTs were dispersed into epoxy resin of one of the specimens for enhancement of stress. We called a specimen without CNTs as 45U, and one with 2wt% of CNTs as 45UV. Schematic image of the textile of the braided carbon-fiber bundles is shown in Fig. 1 (c). The carbon-fiber bundles are continuous from end to end in its longitudinal direction as shown. One bundle in the specimens consists of 12000 carbon fibers, whose diameter is 7 μm. The width of the bundles is roughly 2 mm.

2.2. Tensile testing

In this research, aluminium tabs of 1 mm in thickness were attached on both faces of both ends of the specimens, and step-by-step tensile load was applied in the longitudinal direction of the specimens by using an Instron Universal Testing Machine (Model 4206, Instron) at a crosshead speed of 1 mm/min. To monitor the progress of the destruction on the surface of the specimen, white watercolor was painted on them. Strain gauges were stuck on the surfaces of the specimens to obtain stress-strain curves of the specimens. Fig. 2 shows the stress-strain curves. Pictures of the specimens at certain stages are shown in

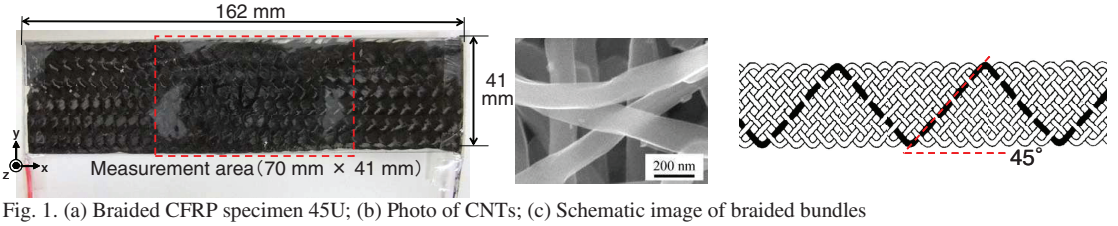

Fig. 1. (a) Braided CFRP specimen 45U; (b) Photo of CNTs; (c) Schematic image of braided bundles

chapter 4. With increasing the tensile loading, the stresses increased nonlinearly in the stress-strain curves in the both specimens. In the case of 45U, the stress was dropped when the strain was 0.055 (see "b" in Fig. 2) due to occurrence of a crack along 45° bundles. However, when the tensile test was resumed, the stress slightly increased. After repeating slight stress increasing and dropping, many bundles of 45U were broken and reached final rupture when the strain was 0.072 ("c"). The stages "a", "b" and "c" in Fig. 2 are defined as "45U before loading", "45U at first stage" and "45U after loading", respectively. On the other hand, fracture behaviour of 45UV was different from 45U. At the stage "e" in Fig. 2, many matrix cracks on the side edges were observed, although the stress did not drop. The stress drastically dropped when the strain was 0.058, and 45UV was broken all of a sudden at "f". The maximum stress of 45UV was 1.3 times higher than that of 45U. The stages "d", "e" and "f" are defined as "45UV before loading", "45UV at first stage" and "45UV after loading", respectively.

3. NDE using SQUID gradiometer

3.1. Measurement method

In order to monitor the conditions of the braided CFRP specimens under the step-by-step tensile test, following SQUID-NDE method was applied to the specimens. By applying a voltage to a board specimen in the *xy* plane, a current is induced in the specimen to generate a magnetic field. The magnetic field gradients (dB_z/dy, dB_z/dx) in a *xy* plane close to the specimen have a relationship with the current densities (J_x, J_y) in the specimen ($dB_z/dy \approx \mu_o J_x$, $dB_z/dx \approx -\mu_o J_y$), according to the Maxwell's equation ($\nabla \times \mathbf{H} = \mathbf{J}$) [5]. Accordingly, the distributions of the field gradients dB_z/dy and dB_z/dx in the *xy* plane above the specimen are analogous to the distributions of the current densities J_x and J_y. In our measurements, after the electrodes were fixed on the left and right ends of the specimens where carbon fibers were naked, currents were induced in all carbon-fiber bundles equally by applying a voltage between both ends of the braided CFRP specimens. Then, the field gradient distributions dB_z/dy and dB_z/dx above the specimen were measured using a HTS-SQUID gradiometer with a small baseline. By this method, one can obtain two-dimensional distributions of the field gradients, which are analogous to the current densities. The condition of the carbon fibers such as breakage and density were evaluated from the distributions.

3.2. Measurement system

A schematic diagram of a measurement system with a HTS-SQUID gradiometer used in this work is shown in Fig. 3. Using this measurement system, the field gradients in the *xy* plane above the specimen were measured while inducing an ac current of 7 mA at 800 Hz in the specimens. In this system, a planer HTS-SQUID gradiometer with two square coils (1 mm × 1 mm), which forms a differential pick-up coil, was employed. The magnetic flux noise of the gradiometer at 800 Hz was about 17 $\mu\Phi_0/\mathrm{Hz}^{1/2}$. The scanning intervals were 1 mm in the *x* and *y* directions and the scanned range was 70 mm × 41 mm. The standoff distance between the gradiometer and the surface of the specimen was 2 mm in the case of the specimen before loading and was 3 mm in the other cases due to the thickness of the tabs.

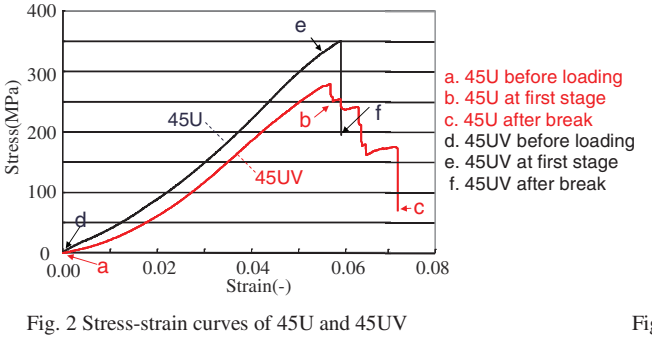

Fig. 2 Stress-strain curves of 45U and 45UV

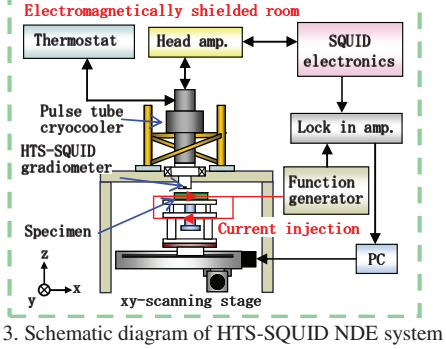

Fig. 3. Schematic diagram of HTS-SQUID NDE system

4. Results and discussion

4.1. Specimen without CNTs (45U)

Figs. 4 (a) ~ (c) show the photos of the specimen 45U at the stages "a" ~ "c" in Fig. 2, and Figs. 5 (a) ~ (c) show the measurement results of dB_z/dy distributions at the respective stages. In all the measurements, the currents flowed from the left to the right in the figures, and black in the figures shows that the field gradient dB_z/dy is higher at the position. As shown in Fig. 5 (a), there are peaks of the gradient above the both edges. On the other hand, there are not large changes in the middle of the specimen compared to the both edges, although there are stripes along the bundles aligning with the angles of ±45°. These stripes were caused by the currents flowing in the bundles with the angles of ±45° [3,4]. We note that there is an area along the line A shown by a broken line, where the field gradient is low.

When the tensile load was applied, a crack with angles of the 45° was occurred around the line A at the stage "b", and the stress dropped. Fig. 5 (b) shows the measurement result of 45U at first stage. The spatial resolution and signal intensity were a bit lower than those in Fig. 5 (a) because the standoff distance was 1 mm longer due to the tabs. Despite the occurrence of the visible crack in the stage "b", the field gradient distribution around the line A in Fig. 5 (b) was roughly same as that in Fig. 5 (a). If some bundles were broken by the crack, the current and field gradient distributions should be changed. Therefore, it is estimated that the crack was a surface matrix crack which did not break on the fibers.

Applying the additional tensile load to the specimen from the stage "b", the matrix crack propagated, and delamination of the matrix and the breakage of the bundles occurred around the line A at the stage "c". As shown in Fig. 5 (c), the field gradient became low in the lower area of the line A. On the contrary, it became high in the upper area of the line A. The results suggest that the current did not flow in the lower right direction, and the current flowed in the upper area of the specimen. From these results, it is estimated that the bundles with the angle of -45° were broken on the line A, and the current detoured the broken site and flowed through the unbroken bundles in the upper area of the line A. It is suggested that the measurement method using the SQUID gradiometer can distinguish between broken bundles and healthy bundles, which is difficult by the surface observation.

To investigate the cause of the surface matrix crack and the final rupture around the line A, where the field gradient was low even at the virgin condition "a", the specimen was cut and the cross-section was

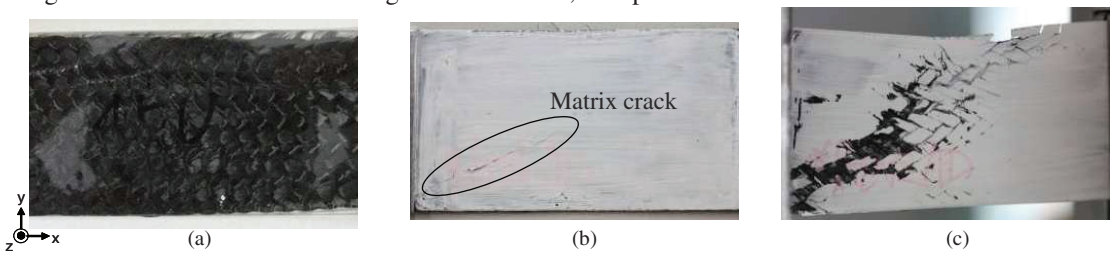

Fig. 4. Photos of ; (a) 45U before loading; (b) 45U at first stage; (c) 45U after break

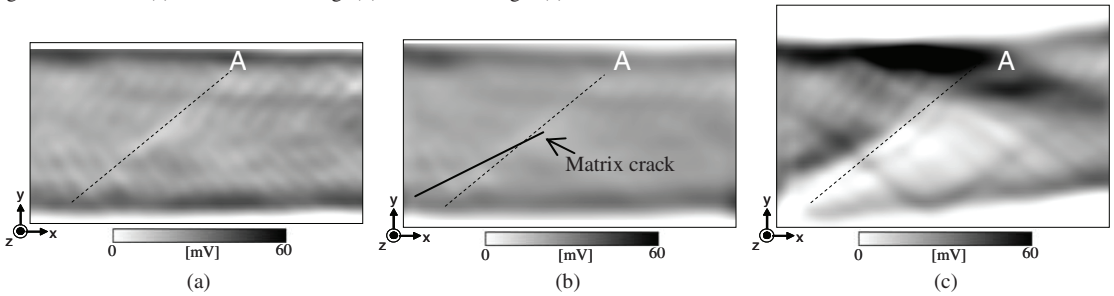

Fig. 5. Distributions of dB_z/dy above specimen; (a) 45U before loading; (b) 45U at first stage; (c) 45U after break

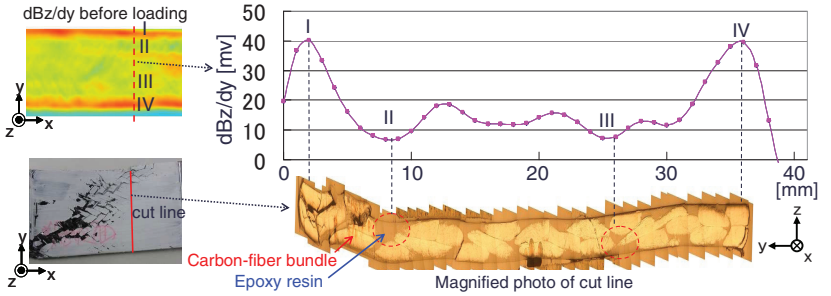

Fig. 6. Cross-section of 45U and profile of field gradient above the cut line before loading

observed. As the breakage was serious near the line A, we cut the right area of the line A, which is indicated in left-hand figures of Figs. 6 by the dotted lines. Figs. 6 show the microscopic photo of the cross-section of the specimen and the profile of the dB_z/dy distribution above the line, which was derived from the result before loading. From the photo, it is found that carbon fibers densely closed up in the both edges, and the densities of carbon-fiber bundles in the resin were not so uniform. Comparing the photo of the cross-section with the profile of dB_z/dy above the cut line, the density of the carbon fibers is high in the both edges I and IV where the dB_z/dy are higher, and the density of the carbon fibers is low at II and III where the dB_z/dy are low. The result suggests that the area around line A has low carbon-fiber density. From the results, when the tensile loading was applied to the braided CFRP, there is a possibility that the matrix crack occurred at the low field gradient area around the line A where the density of the bundles is estimated to be low, and the breakage progressed by concentration of the stress at the area.

4.2. Specimen with CNTs (45UV)

Figs. 7 (a) ~ (c) show the photos of specimen 45UV at the stages “e” ~ “f”, and Figs. 8 (a) ~ (c) show the measurement results of dB_z/dy distributions. As shown in Fig. 7 (a), compared to 45U, the field gradient above the both edges are higher and that is lower in the middle of 45UV before loading. As making conditions of 45U and 45UV were same except for CNTs, the phenomenon occurred due to CNTs. Since CNTs have high conductivity, it is considered that CNTs placed between carbon fibers lowered the contact resistance between the fibers. As shown in the photo of cross-section in Fig. 6, as the bundles in the turning part of flat braided CFRP densely closed up, contact area of the bundles near the edges were larger than that in the middle of the specimen. Therefore, the resistance between the bundles became lower due to CNTs especially near the edges, and the current transmitted between the bundles near the edges. From this result, it is suggested that CNTs combined carbon fibers electrically. Moreover, because of improvement of the maximum stress and the change of fracture appearance, it is considered that CNTs changed the mechanical characteristic of the braided CFRPs. Furthermore, a few lines where the field gradient is low were detected as with 45U, which are indicated by the dotted lines in Fig. 8 (a).

Applying the tensile load to the 45UV, the matrix crack occurred at the lower area of the specimen at the stage “e”. However, as there was no large change in the gradient distribution between 45UV before loading in Fig. 8 (a) and at first stage in Fig. 8 (b), there were only matrix cracks. Applying the additional tensile load to the 45UV from the stage “e”, the stress of the 45UV increased to the maximum, and then 45UV broke suddenly. It is observed that most of the bundles were broken from the appearance shown in Fig. 7 (c). From the field gradient distribution in Fig. 8 (c), the field gradient became high in the upper area of the 45UV, and several high field gradient lines along some bundles were observed in the lower area. From the results, current flowed in the unbroken bundles in 45UV at the stage “f”.

Since matrix cracks were observed in the lower area of 45UV as shown in Fig. 7 (b) and the continuous bundles remained in the upper area more than the lower area, it is considered that the fracture started from the lower area of the 45UV. Different from 45U, the fracture progressed in a dogleg shape in

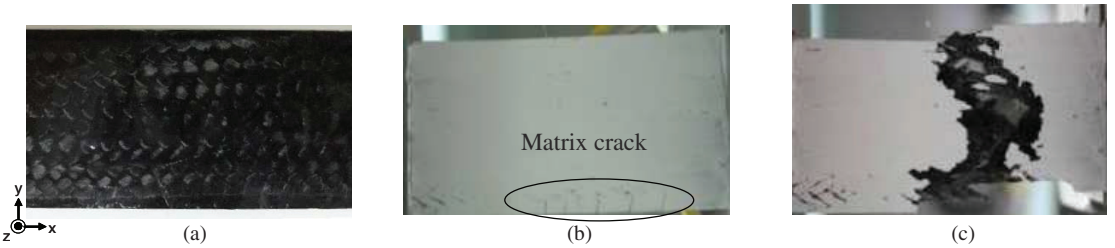

Fig. 7. Photos of; (a) 45UV before loading; (b) 45UV at first stage; (c) 45UV after break.

.

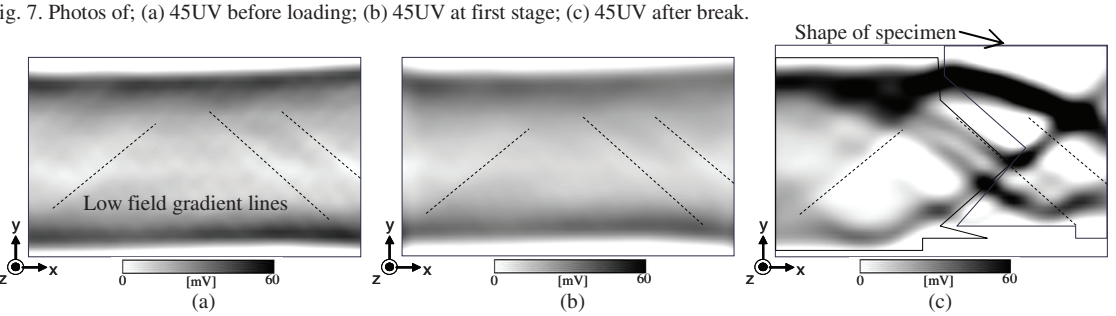

Fig. 8. Distributions of dB_z/dy above specimen; (a) 45UV before loading; (b) 45UV at first stage; (c) 45UV after break

45UV as shown in Fig. 7 (c). The upper part of the rapture corresponded to the one of the lines, where the field gradient was low. As we mentioned before, it is estimated that the low field gradient line should correspond to the area where the density of the carbon fibers is low, and the propagation of the crack might occur along the line. From the results, it is estimated that the line where field gradient is low tends to be a broken site in the braided CFRP specimen with CNTs as well as 45U. From the results of the two specimens, it is indicated that there is a possibility to predict the initiation site of destruction in braided CFRPs by the SQUID-NDE method even before any load is applied.

5. Summary

We applied the step-by-step tensile test and current-injection-based NDE method using the HTS-SQUID gradiometer to the braided CFRPs with and without CNTs. In the measurement results, the changes of the current distribution due to the fractures of the specimens and due to the inclusion of CNTs were successfully observed. Furthermore, low field gradient lines were detected before loading, and the lines corresponded to the breakage sites of the specimens after loading. From these results, we showed that the validity of the method to evaluate the conditions of the carbon fibers in the braided CFRPs and the possibility to predict the initiation site of destruction of the braided CFRPs.

References

[1] Falzon PJ, Herszberg I. Mechanical performance of 2-D braided carbon/epoxy composites. *Compos Sci Technol* 1998;**58**:253-65.
[2] Fujihara K, Huang ZM, Ramakrishna S, Satknanantham K, Hamada H. Performance study of braided carbon/PEEK composite compression bone plates. Biomaterials 2003;**24**:2661-7.
[3] Shinyama Y, Hatsukade Y, Tanaka S, Takai Y, Aly-Hassan MS, Nakai A, Hamada H. Nondestructive Evaluation of Braided Carbon Fiber Composites Using High Tc SQUID. *Adv Mater Res* 2010;**123-125**:835-8.
[4] Shinyama Y, Hatsukade Y, Tanaka S, Takai Y, Aly-Hassan MS, Nakai A, Hamada H. Nondestructive Evaluation of Braided Carbon Fiber Composites with artificial defect Using HTS-SQUID gradiometer. *Physica C*, in press, 2011.
[5] Hatsukade Y, Aly-Hassan MS, Kasai N, Takashima H, Hatta H, Ishiyama A. SQUID-NDE method on damaged area and damage degree of defects in composite materials. *IEEE Trans Appl Supercond* 2003;**13:**207-10.
[6] Hatsukade Y, Inaba T, Maruno Y, Tanaka S. Mobile cryocooler-based SQUID NDE system utilizing active magnetic shielding. *IEEE Trans Appl Supercond* 2005;**15**:723-8.
[7] Hatsukade Y, Takahashi T, Yasui T, Tsubaki M, Fukumono M, Tanaka S. Study on nondestructive inspection using HTS-SQUID for friction stir welding between dissimilar metals. *Physica C* 2007;**1038**:463-5.